

Céramiques imprimées de Méditerranée occidentale (VI^e millénaire AEC) : données, approches et enjeux nouveaux / Western Mediterranean Impressed Wares (6th millennium BCE):

New data, approaches and challenges

Actes de la séance de la Société préhistorique française de Nice (mars 2019)

Textes publiés sous la direction de Didier BINDER et Claire MANEN

Paris, Société préhistorique française, 2022

(Séances de la Société préhistorique française, 18), p. 307-326

www.prehistoire.org

ISSN : 2263-3847 – ISBN : 2-913745-89-X

Characterization and study of the provenance of ceramics using portable X-ray fluorescence (pXRF): test study on terrae with granitic and metamorphic components from Castellar – Pendimoun (Impressa and Cardial, 6th millennium BCE)

Damase MOURALIS, Chrystèle VERATI, Gilles DURRENMATH,
Jean-Marc LARDEAUX and Didier BINDER

Résumé : Depuis de nombreuses années, les études de provenance des terres utilisées en céramique, parmi d'autres archéomatériaux, se multiplient afin de documenter les transferts de matières premières ou d'artefacts. Avec la pétrographie et la minéralogie, la géochimie contribue à la caractérisation des terres et à l'identification des sources de matière première afin de produire des hypothèses concernant l'origine et la diffusion de la production de la céramique.

Plus récemment, ces études de provenance ont bénéficié de la miniaturisation des analyseurs et de l'apparition d'appareils portables à fluorescence X (XRF portable), abondamment utilisés pour caractériser une grande diversité de matériaux et d'artefacts archéologiques (lithiques, céramiques, métaux, etc.). Grâce à leur portabilité, ces appareils offrent la possibilité d'analyser les artefacts *in situ* (dans les musées, sur les fouilles ou sur le terrain) en limitant ainsi les difficultés administratives associées à l'exportation du matériel archéologique. Il est alors possible d'étudier un grand nombre d'artefacts et de proposer une approche quantitative, plus représentative de la diversité potentielle des sources exploitées.

Relativement faciles à utiliser par des scientifiques qui ne sont pas d'abord des géochimistes (géographes, archéologues, géologues, etc.), ces appareils sont parfois utilisés comme des « boîtes noires » à l'intérieur desquelles les utilisateurs n'interviennent pas. Ils laissent alors l'appareil opérer une déconvolution automatique des spectres X et ne questionnent pas la précision analytique. Dans ce contexte, cet article discute l'intérêt et les limites de la fluorescence X portable pour caractériser les céramiques.

Nous soulignons tout d'abord la nécessité d'un protocole analytique robuste. Il est primordial d'utiliser des standards afin de contrôler la précision de l'appareil. L'utilisation répétée de ces standards permet également de vérifier la stabilité et la répétabilité des mesures analytiques. Dans la mesure du possible, ces standards doivent présenter une gamme de concentration élémentaire similaire à celle du matériau étudié. Il peut s'agir de matériaux de référence certifiés (CRM) vendus par divers bureaux internationaux ou de standards « internes » (*in-house standards*) analysés indépendamment à l'aide de méthodes de laboratoire robustes (par exemple ICP-MS ou ICP-AES, etc.). Dans la présente étude, les standards internationaux sont six CRM fournis par le SARM (France) et les standards « internes » sont composés de vingt « terres d'intérêt » correspondant aux trois sources potentielles du piémont de l'Orméa ($n = 3$), du massif des Maures-Tanneron ($n = 9$) et du massif de l'Argentera-Mercantour ($n = 8$). Toutes ces terres d'intérêt ont été cuites à 700°C afin d'approcher l'état des céramiques étudiées.

Afin de tester la capacité de l'appareil à différencier les sources de matériaux, cet article présente les analyses XRF portables de vingt-et-un tessons appartenant à dix-sept céramiques découvertes sur le site de Pendimoun et étudiées dans le cadre du programme CIMO (tabl. 1 ; Gabriele *et al.*, ce volume; Lardeaux *et al.*, ce volume). Quinze céramiques appartiennent à l'*Impressa* (phases PND-1A, 1B) et deux au *Cardial* (phase PND-2). Les recherches précédentes ont démontré que les céramiques de Pendimoun utilisent trois pâtes différentes. La pâte glauconieuse du Crétacé (GL) est facilement accessible sur les contreforts de l'Orméa, à proximité immédiate du site. Un deuxième groupe de pâtes, nommé quartz-micas-feldspath (QMF), provient soit de l'Argentera-Mercantour, soit du massif des Maures-Tanneron. Le dernier groupe correspond à un mélange des deux pâtes (MIX). Les dix-sept céramiques étudiées dans cet article appartiennent toutes au groupe QMF et, sur la base des analyses pétrographiques et géochimiques précédentes, sont originaires de l'Argentera-Mercantour ($n = 7$), des Maures-Tanneron ($n = 1$) et du QMF indifférencié ($n = 9$; tabl. 1).

Sur la base des analyses des « terres d'intérêt », l'article démontre la capacité de l'appareil à détecter une large gamme d'éléments présents dans les céramiques et généralement considérés comme « majeurs » (Al, Si, K, Ca, Fe, P, Mg), « mineurs » (Mn) et « traces » (Ni, Rb, Zr, Sr, Y, Ba, Nb, Pb, Th, Co, Zn, Ni, Sn, Ta) (tabl. 2). De plus, la comparaison entre les valeurs attendues et les valeurs mesurées (fig. 2) pour les CRM et les « terres d'intérêt » indique une très bonne capacité de l'analyseur à mesurer dix-sept éléments dans des gammes de concentration allant de quelques dizaines de % (Si) à quelques parties par million (Zr par exemple). Le coefficient de corrélation R^2 est supérieur à 0,99 pour Mg, Ca, Fe, Zn, Sr, Zr, Ba et est compris entre 0,949 et 0,99 pour Si, P, K, Mn, Ni, Nb, Rb, Sn, Ta et Th (tabl. 4).

Le diagramme SiO_2 vs Al_2O_3 (fig. 6) démontre que l'appareil est capable de distinguer les trois principales sources de matériaux. Sur ce même diagramme (SiO_2 vs Al_2O_3), la plupart des tessons ($n = 15$) sont situés près du champ occupé par les « terres d'intérêt » de l'Argentera-Mercantour (fig. 7). Sur le diagramme ternaire Fe_2O_3 , Al_2O_3 , SiO_2 (fig. 8), les tessons sont également regroupés autour des TI de l'Argentera-Mercantour. Seuls deux tessons occupent une position intermédiaire entre les sources Maures-Tanneron et Argentera-Mercantour. Le *sourcing* réalisé avec l'analyseur portable XRF est donc cohérent avec les résultats minéralogiques, pétrographiques et géochimiques obtenus précédemment dans le cadre du programme CIMO (tabl. 1).

Afin de tester l'hypothèse d'un mélange de terres (QMF et GL) dans un même vase, des transects longitudinaux et équatoriaux ont été réalisés pour deux céramiques particulièrement bien conservées avec respectivement seize et vingt-deux mesures le long de chaque transect. Pour la première céramique, les résultats ne révèlent pas d'hétérogénéité géochimique spatiale significative, suggérant que ce vase a été construit principalement à partir de la terre du massif de l'Argentera-Mercantour. En revanche, pour la seconde céramique, le transect montre une forte variabilité de trois éléments principaux, le calcium (Ca), le phosphore (P) et le potassium (K).

Nous faisons l'hypothèse que cette variabilité est corrélée à des effets taphonomiques plutôt qu'à une réelle hétérogénéité des pâtes. En effet, le calcium est particulièrement mobile et abondant dans un contexte d'abri rocheux ouvert dans le calcaire. Le phosphore est un élément associé à la matière organique et à l'occupation humaine de l'abri sous roche. La variation de la teneur en K pourrait être liée à sa mobilité relative dans les conditions d'altération. Elle pourrait également être associée à la présence de phénocristaux de feldspath riches en potassium sous le point de mesure. La porosité associée à de larges pores (1 à 50 µm) démontrée ailleurs (Drieu *et al.*, 2019) pourrait favoriser une pollution des tessons par des éléments mobiles. Ceux-ci proviendraient soit de l'altération des roches carbonatées, soit de la redistribution de sucs organiques liés à l'utilisation de l'abri comme bergerie.

Enfin, la présente étude démontre la capacité de l'appareil portable à sourcer correctement les céramiques si deux conditions sont respectées. Premièrement, les analyses chimiques doivent respecter un protocole robuste basé sur l'utilisation répétable de CRM et de standards « internes ». Deuxièmement, l'étude doit s'insérer dans une démarche combinant des méthodes complémentaires (pétrographie, minéralogie et géochimie de laboratoire). Dans ces conditions, l'utilisation de l'analyseur portable permet de réaliser des études non destructives sur un nombre important de céramiques dans un laps de temps relativement contraint et de distinguer rapidement les principales sources.

Mots-clés : géoressources, pâtes granitiques, fluorescence X, analyseur portable.

Abstract: In recent years, the use of portable X-ray fluorescence analysers (portable XRF) has developed considerably, particularly for characterising archaeological materials (lithics, ceramics, metals, etc.). Because of their portability, these devices offer many advantages, including the possibility of analysing artefacts *in situ* (in museums, on excavations or in the field) avoiding the difficulties of exporting archaeological material. Portable XRF allow thus to characterise a large number of artefacts during a limited time. Relatively easy to use, these devices are sometimes used as a “black box”, with no or poor user control. In this context, this article discusses the interests and limitations of portable X-ray fluorescence for characterising ceramic bodies.

The article first highlights the need to use standards (CRM and/or in-house standards) to control the accuracy of the instrument for the different chemical elements studied and their concentration range. The article then takes the example of the ceramics and raw material sources (*terres d'intérêt*) studied in the framework of the CIMO programme and concludes that it is possible to distinguish the main sources of the materials used for the ceramics from the Pendimoun site. Finally, our paper underlines the complementarity of the approaches. Portable XRF geochemistry allows a relatively rapid and non-destructive analysis of a large number of sherds. But the analysis of these results becomes more robust when it is based on prior knowledge (geochemical, mineralogical and petrographical) of the potential sources.

Keywords: geological sources, granitic pottery pastes, X-ray fluorescence, portable device.

CHARACTERIZING AND SOURCING CERAMIC TERRAE: SCIENTIFIC SETTINGS AND AIMS OF THE STUDY

For many years, geochemistry has been used for the characterisation of pastes and for producing hypotheses concerning the origin and diffusion of ceramics. The characterisation of pastes and the identification of sources are thus part of a current of research on archaeomaterials, the results of which make it possible to document the transfer of raw materials or artefacts as well

as the mobility of the populations themselves. Classically implemented for historical periods (*inter alia*, Maggetti, 1981 and 1986; Picon and Le Mièvre, 2002; Laviano and Muntoni, 2007; Schmitt *et al.*, 2009; Eramo *et al.*, 2018), major and trace element analysis has also been developed for the Neolithic, especially when pastes include rare and/or very small non-plastic particles making their petrological and mineralogical characterisation under the microscope more delicate (*inter alia* Basso *et al.* 2006; Laviano and Muntoni, 2006; Muntoni and Laviano, 2008; Muntoni and Eramo, 2016; Stapfer *et al.*, 2019).

Within the framework of the CIMO project, geochemical analyses are part of an integrated methodology including petrography and mineralogy of the pastes and their constituents following a naturalistic approach. Within the CIMO project, geochemistry has provided particularly robust data for the demonstration of long-distance transfers in the Western Mediterranean basin as early as the Neolithic. For example, Binder and colleagues (Binder *et al.*, 2018) have demonstrated the presence of the Southern Italian *Serra d'Alto* productions at Saint-Benoit (cave 2 of la Lare, Alpes-de-Haute-Provence) in the extreme end of the 6th / first half of the 5th millennium BCE. In a similar way, Gabriele and colleagues (Gabriele *et al.*, 2019) have identified in the Mediterranean Languedoc at Portiragnes (Pont-de-Roque-Haute, Hérault) early *Impressa* ceramics originating from the Tosco-Latian volcanic province and dated to the first half of the 6th millennium. Lastly, the contribution of geochemistry has been decisive in characterising the “granitic” pastes originating from the Argentera-Mercantour and their diffusion during the *Impressa* (Castellar – Pendimoun, Lardeaux *et al.*, this volume).

The use of portable X-ray fluorescence analysers (portable XRF, pXRF), which has increased over the last decade, offers the possibility of studying a large number of artefacts without destroying them, whereas more invasive geochemical analyses processed on powder can only analyse a limited number of samples. In addition, taking advantage of their portability, these devices can be used in the field, on excavation or in the museum and they avoid the administrative constraints specific to the export of archaeological materials. These benefits explain that these devices are increasingly integrated into research programs dedicated to the characterisation of archaeological materials (Liritzis and Zacharias, 2011).

Portable XRF devices have been widely used for the characterisation of obsidian artefacts and the identification of the sources. Hyaline material is indeed “an ideal material” for such analyses for three main raisons. It is a homogeneous material, it comes from well-identified and quite limited volcanic sources, and each volcanic source gets a specific chemical fingerprint (for a recent review, see Mouralis, 2016). Moreover, during the last decade, the use of portable X-ray fluorescence has also developed to characterise other material than ceramics (*e.g.* Stapfer *et al.*, 2019; Belfiore *et al.*, 2014; Forster and Grave, 2012).

In general, the widespread use of portable analysers by researchers who are not primarily geochemists has led to scientific controversy. For example, R. J. Speakman and M. S. Shackley (Speakman and Shackley, 2013) criticize E. Frahm (Frahm, 2013) for “silo science”, *i.e.* for producing obsidian characterisation data using a portable analyser that do not meet geochemical standards and are therefore not comparable to those obtained by laboratory methods. As a matter of fact, recent papers on pXRF characterisation of ceramics focus on methodology (Stapfer *et al.*, 2019) or on the use of reference material (Frahm *et al.*, 2022).

As the amount of researches on ceramic pastes using p-XRF has increased dramatically over the past two

decades, it is necessary to assess the validity of its application. For this purpose, the present article has a double goal. The first one is to present the interest and the limits of the use of portable X-ray fluorescence to characterise ceramic pastes and to discuss the analytical protocol that can be implemented. The second objective is to precise how it is possible to identify the sources of ceramic pastes, *i.e.* to relate them to a known and previously characterised geological source of terrae. This second question refers in turn to the possibility of detecting the presence of several sources in the same ceramic as well as to discuss potential effects related to the taphonomic conditions and their impact on initial chemical characteristics.

METHOD USED AND MATERIAL STUDIED

Advantages of portable X-ray fluorescence

Portable X-ray fluorescence is increasingly used in archaeology because of several advantages, among which we should mention at first portability, which allows for in-situ analysis and removing some of the administrative issues for exporting archaeological material; second, versatility, which allows for the analysis of a wide variety of materials, including rocks, sediments, terrae, or metals; third, non-destructive X-ray fluorescence analysis; and lastly, the very low cost of analysis, once the initial investment is made through the purchase of the apparatus.

Principles of X-ray fluorescence (XRF) and calibration

X-ray fluorescence occurs when the X-rays reach the rock or other material: the material re-emits energy, notably in the form of “secondary” X-rays, the spectrum of which is characteristic of the composition of the sample. For each energy line (expressed in keV), the analyser’s detector records an intensity (expressed in counts per second). Each chemical element is characterised by a set of energy lines. Software can then identify the various chemical elements contained in the sample according to the characteristic lines (a process often called “deconvolution” of the signal). Finally, the software associates the intensity of the lines with the elemental concentration (expressed in ppm or %). This last step is highly dependent on the calibration of the instrument.

There are different types of calibration (Shackley, 2011). The FP (fundamental parameters) method uses mathematical algorithms that describe the response of the detector when the X-ray encounters pure elements. Empirical calibration is based on the use of international standards, analysed in different laboratories and whose concentrations are certified (certified reference materials, hereafter abbreviated CRM). In this case, the operator measures the CRM contents using the portable XRF analyser and compares them with the certified values to identify the correction factors to be introduced in the software.

Laboratory (or “benchtop”) instruments are never calibrated by the manufacturer. For these devices, the operator is responsible for calibration (Hunt and Speakman, 2015) and must therefore use the fundamental parameters and/or CRMs. In contrast, portable devices are generally sold “ready to use” offering a “factory” calibration that comes in different modes (ores, soils, etc.) approximating the types of materials the user may encounter.

Thus, in most cases, portable XRF instruments behave like “black boxes”, as the manufacturers do not provide access to the algorithms for identifying elements and their concentration. On the other hand, it is possible to introduce correction parameters that are added to the “factory”

calibration and come close to an empirical calibration using CRMs. Before performing the calibration, it is useful to check to what extent the “factory” settings are correct, by comparing the measured values with reference values.

Two additional points have to be taken into account. Firstly, the CRMs should be as closed as possible from the analysed material: they should contain the same chemical elements with comparable concentrations. This proximity will ensure the accuracy of the model (Hunt and Speakman, 2015). Secondly, in X-ray fluorescence, the intensity of a ray is not directly proportional to the concentration of the chemical element as some of the characteristic lines overlap. Thus, the other elements within

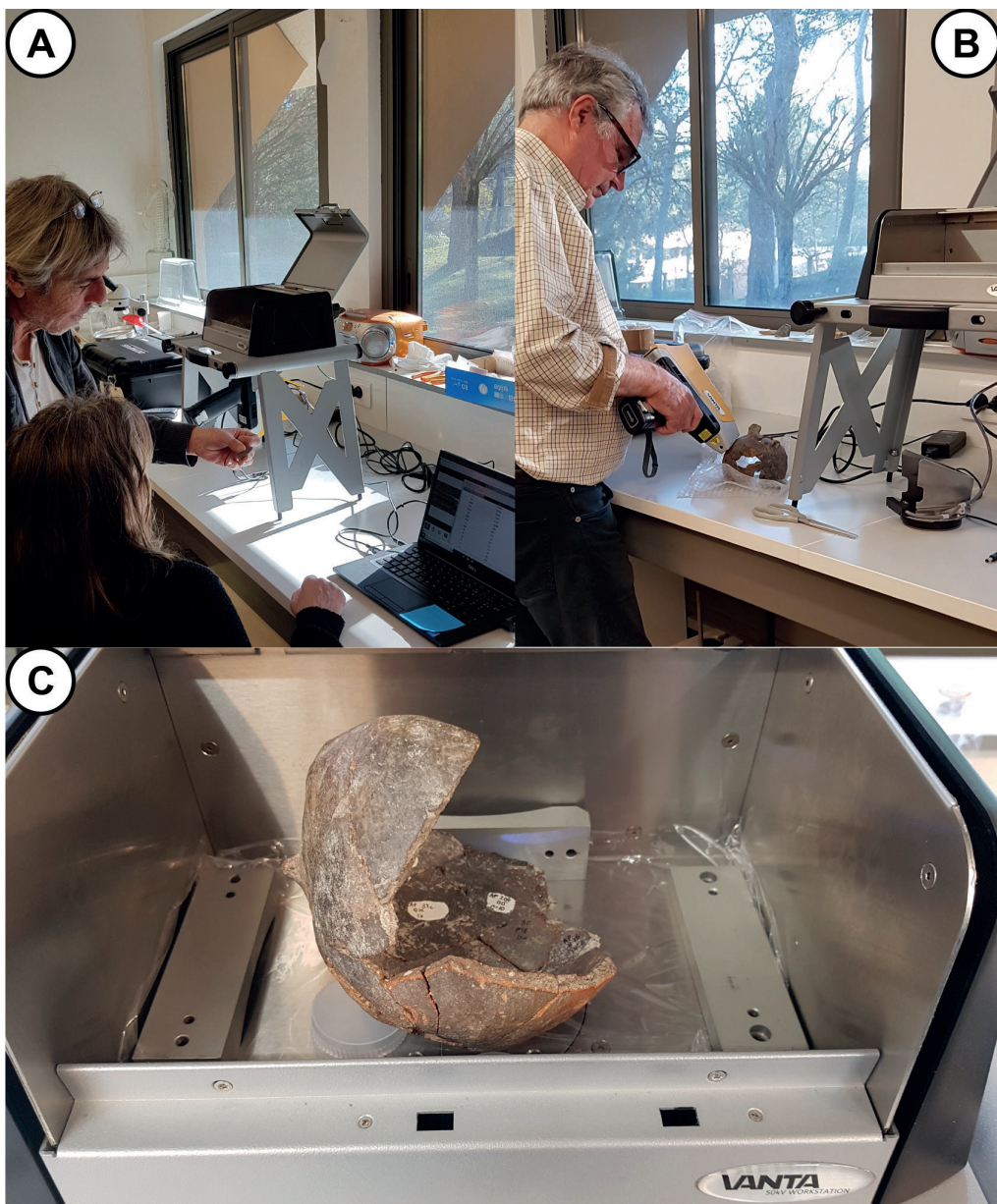


Fig. 1 – Photographs of the analytical device. A: use of the Vanta portable XRF under the measurement stand and driven by a laptop. **B:** use of the portable device “freehand” on a ceramic the shape of which makes it impossible to enter the measuring stand. **C:** the measuring stand and the AP001 ceramic.

Fig. 1 – Photographies du dispositif analytique. A : utilisation de l’XRF portable Vanta asservi sous le stand de mesure et piloté par un ordinateur portable. **B :** utilisation de l’appareil portable « à main levée » sur un tesson dont la forme ne permet pas son installation dans le stand de mesure. **C :** le stand de mesure et le tesson AP001.

the sample contribute to the overall signal: this is known as the “matrix effect”. It is therefore necessary to calibrate the apparatus using materials whose elemental contents are as close as possible to the samples studied.

The international standards used (CRM) have matrices different from the ceramic bodies we wish to analyse for this study. Therefore, in order to control the quality of the “factory calibration” of the portable analyser, we used not only CRMs but also in-house (or internal) standards from experimental ceramics made with the probable sources of terrae and named in the CIMO project “*terres d'intérêt*”, hereafter abbreviated to TI (fig. 1). These terrae had previously been analysed using another method (e.g.

ICP-MS) considered as a reference method. It is then possible, as with the CRMs, to compare the expected and measured values and thus to control the measurements from the portable device, or even to calibrate it. These internal standards have the advantage of having the same concentration ranges and the same matrix effects as the ceramic terrae to be analysed.

Apparatus and analytical conditions

The analyser used is a VANTA VMR model manufactured by Olympus and acquired by the GEOAZUR Laboratory in the framework of the CIMO programme.

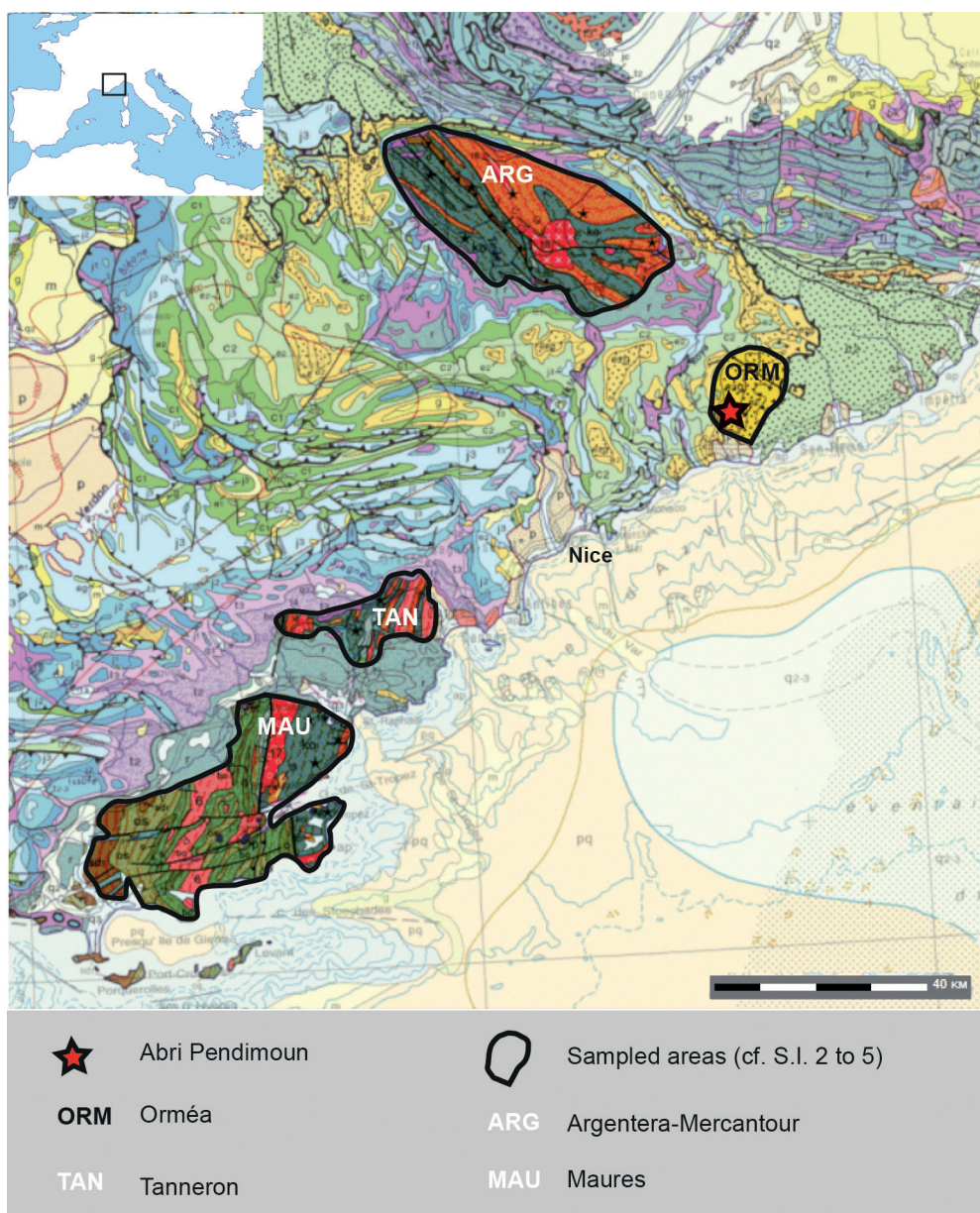


Fig. 2 – Geological map of the study region with the location of Pendimoun rock shelter and the selected terrae (TI) sampled within their structural contexts. The precise locations of the TI are presented in SD 2 to 5.

Fig. 2 – Carte géologique de la région d'étude : l'abri Pendimoun et les terres d'intérêt (TI) échantillonnées dans leurs contextes structuraux. Les localisations précises des terres d'intérêt sont présentées dans les DS 2 à 5.

This apparatus contains a rhodium (Rh) anode in a 4W tube with a voltage of 50kV. The diameter of the beam is approximately 7mm and its surface area is 40mm². We opted for an analysis time of 60s for light elements and 60s for heavy elements, *i.e.* 120s in total. The analyses were conducted using the “Geochem-REE-extra” mode, which includes a factory calibration based on the fundamental parameters and which the user can correct using an “empirical calibration”.

The analysed materials come in two different forms. Firstly, the certified materials (CRM) and the in-house standards (*terres d'intérêt* or TI) are in the form of powders. Each sample was placed in a pillbox of about 2.5cm diameter, filled to a thickness of 0.5 to 1cm and covered with a 4µm thick Fluxana® TF240-355 polypropylene film. These samples were analysed using the dedicated stand (“VANTA workstation”). Secondly, the archaeological ceramics are shards of varying shapes and sizes. Depending on their size, they were analysed either with the stand or without (freehand; fig. 2).

Analyses of TI and ceramics using the portable analyser

The analyses were carried out in two sessions, in February and July 2019. Six CRM standards were analysed twice each to check the accuracy of the measurements (figs. 3 to 5). Twenty TI samples, fired at 700°C beforehand, were analysed by ICP-MS (fig. 3, SD.1 and SD.2 to 5) in order to check the importance of the matrix effect. Seventeen ceramics from the *Impressa* (n = 14) and Cardial (n = 3) phases of Castellar – Pendimoun were analysed (table 1), with at least two measurements for each of the samples studied. Two ceramics, AP001 and AP045, were respectively analysed in sixteen and twenty-two longitudinal and equatorial transects, in order to highlight possible heterogeneities of the pastes used. For four of the seventeen vases analysed in this study, two sherds were analysed, making a total of twenty-one studied sherds.

One hundred and twenty-nine analyses were carried out using the portable XRF analyser (SD.6). They include the contents of twenty-one chemical elements for which we consider the measurements to be reliable (see table 2). The mean and standard deviation of the CRMs and ceramics for which several analyses were carried out are given in SD.7).

Impresso-Cardial ceramics from Castellar – Pendimoun

The *Impresso-Cardial* ceramics from Castellar – Pendimoun have been the subject of extensive studies combining petro-mineralogical (mesoscopic, *i.e.* stereoscope up to x50 and microscope in unanalysed polarised light LPNA or polarised-analysed light LPA up to x200) and geochemical characterisation methods (Gabriele, 2014; Gabriele *et al.*, this volume; Lardeaux *et al.*, this volume)

These 158 ceramics (table 3) refer to the *Impressa*, phase 1A (n = 20) and phase 1B (n = 84) as well as to the Cardial phase 2 (n = 54). The majority of the production was made in glauconitic marl and clayey sediments (hereafter GL) dated to the Cretaceous, easily accessible on the foothills of the Ormée in the immediate vicinity of the site: 7/20 in phase 1A and 42/84 in phase 1B of the *Impressa*; 43/54 in phase 2 of the Cardial. This type of GL ceramics was not analysed in our study.

The ceramics analysed in this study have been made using pastes with non-plastic inclusions (quartz-mica-feldspar group, hereafter QMF) and represent a minority of the vases identified in the *Impressa* (8/20 in phase 1A, 12/84 in phase 1B) and Cardial (5/54 in phase 2) contexts. The previous petro-mineralogical analyses have shown that the corresponding pastes come from the alteration of crystalline granitic and metamorphic formations, mainly from the Argentera-Mercantour massif and very marginally from the Maures-Tanneron massif.

A last group, different from the GL and QMF, is made up of mixed pastes (hereafter abbreviated to MIX) presenting inclusions characteristic of the two previous groups: 5/20 in phase 1A and 30/84 in phase 1B of the *Impressa*; 6/54 in phase 2 of the Cardial (table 3).

For the present study, seventeen vases from the QMF group were specifically selected. The pastes used were attributed as follows: seven to the Argentera-Mercantour massif, one to the Maures-Tanneron massif and nine to the generic QMF group (table 1). This attribution is based on systematic mesoscopic observations prior to the preparation of thin sections on a limited number of samples. Thus, of these seventeen vases, seven were attributed on the basis of a double meso- and microscopic examination to the Argentera-Mercantour domain and one to the Maures-Tanneron domain, while nine were attributed to the undifferentiated QMF group on the sole basis of binocular examination. In addition, three of them belonging to the *Impressa* QMF family (samples AP001, AP011 and AP028) benefited from a global chemical analysis at the SARM of Nancy in addition to the microscopic observation in thin section (table 1). The seventeen ceramics that form the corpus of the present study were subjected to two analysis sessions using the XRF-portable in February and July 2019 (SD.6, SD.7).

Checking the accuracy of the analyser: internal standards and CRMs

In order to control the accuracy of the instrument, two types of materials were used. Firstly, six CRMs from the *Service d'analyse des roches et minéraux* (SARM) of the *Centre de Recherches Pétrographiques et Géochimiques* (CRPG), located in Nancy (France), were analysed using a dual strategy. In order to use certified materials with elemental contents close to the analysed terrae, three granite CRMs (Granit-GA, -GH and -GS-N) were chosen. In addition, in order to control the measurements of the instrument with a wide range of grades, three other CRMs were used: a poorly differentiated rock (Basalt BR) and

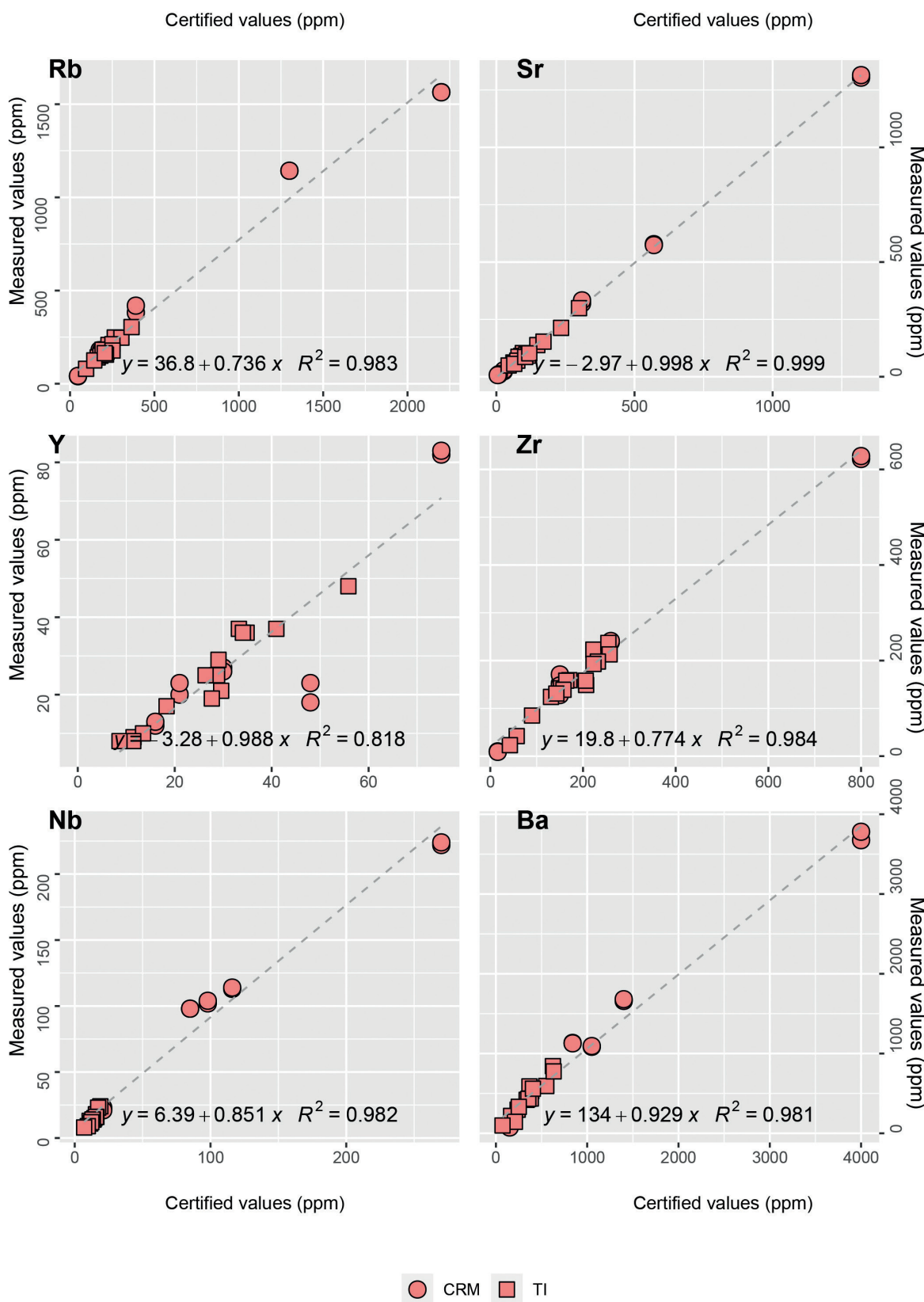


Fig. 3 – XRF-portable analyses of CRM provided by CRPG-SARM and terrae samples heated at 700° C. Expected vs. measured values for some chemical elements (Ba, Nb, Zr, Y, Rb and Sr). Note the very good correlation coefficients (except for yttrium) for various concentration ranges. All correlation coefficients for the twenty-one elements considered in this study are provided in table 4.

Fig. 3 – Analyses par XRF-portable des CRM fournis par le CRPG-SARM et des TI chauffées à 700° C. Valeurs attendues vs valeurs mesurées pour quelques éléments chimiques (Ba, Nb, Zr, Y, Rb et Sr). Remarquez les très bons coefficients de corrélations (à l'exception de l'yttrium) pour des gammes de concentration très variables. Les coefficients de corrélation pour les vingt-et-un éléments pris en compte dans cette étude sont donnés dans le tableau 4.

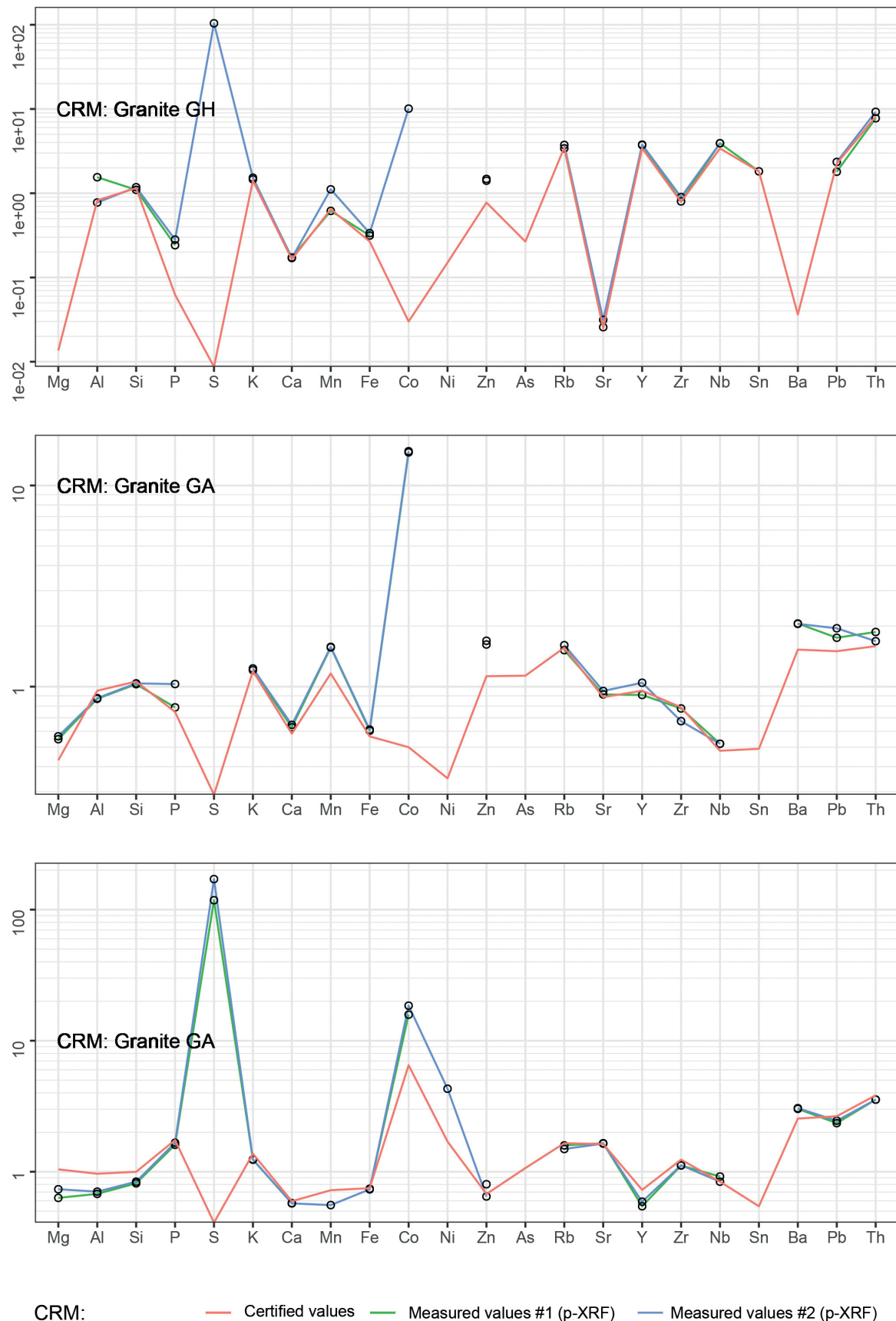


Fig. 4 – Expected (certified) and measured (portable XRF) values for three granitic CRMs. Values normalized to the upper continental crust (Taylor and McLennan, 1995).

Fig. 4 – Valeurs attendues (certifiées) et valeurs mesurées (XRF-portable) pour trois CRM granitiques. Valeurs normalisées à la croûte continentale supérieure (Taylor et McLennan, 1995).

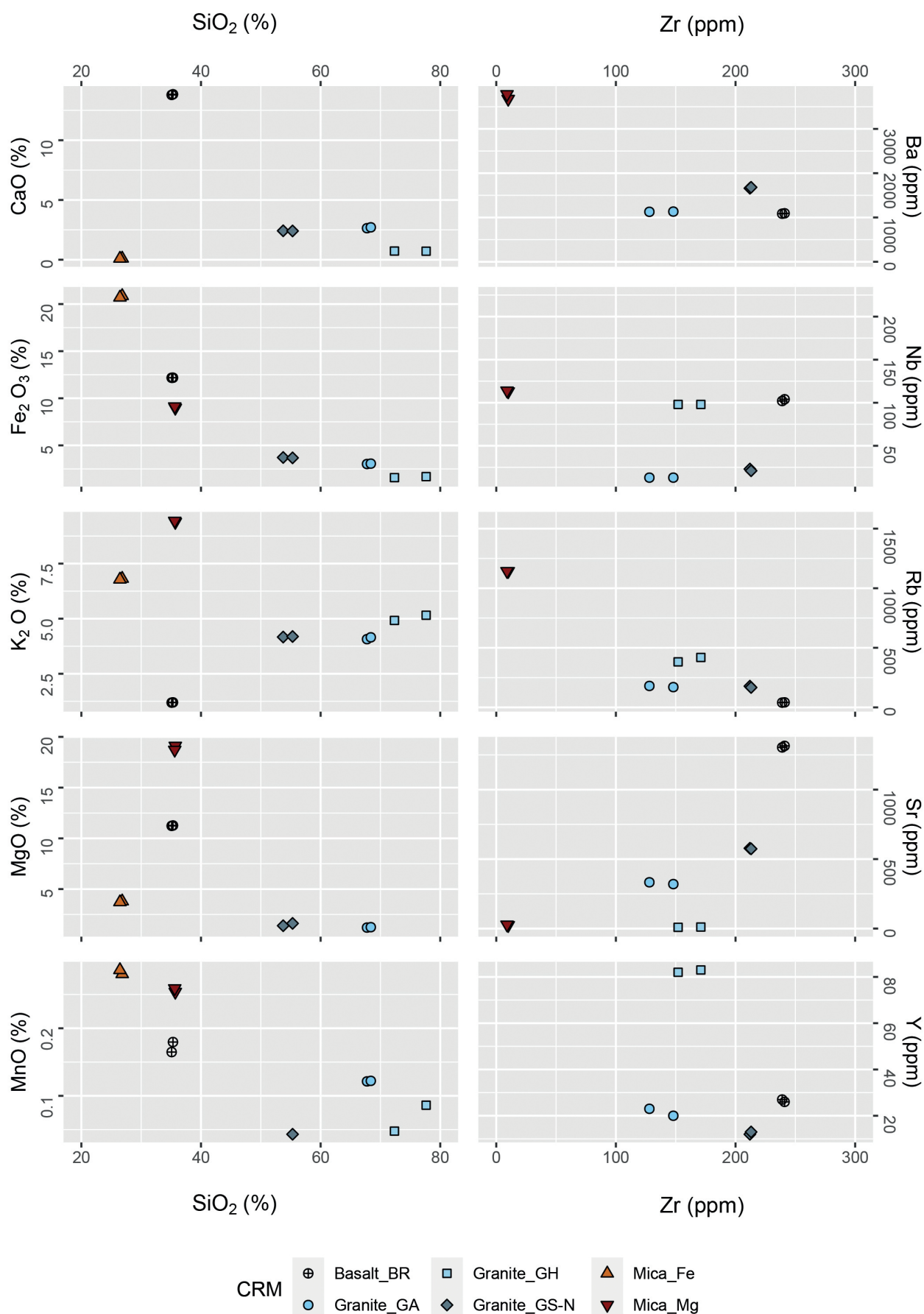


Fig. 5 – Multi-element plots of CRM analyses acquired with the portable-XRF device.
Fig. 5 – Diagrammes multiélémentaires des analyses des CRM réalisées à l'aide de l'appareil XRF-portable.

ID	Sherds	Ceramics			Analyses (CIMO project)			Ceramic features			Petrographic group
		Chemistry (ICP)	Petrogr. (thin section)	CT-Scan	Culture (phase)	Shape	Decoration	Surface deposit			
AP_001	-	Yes	Yes	Yes	Impressa (PND1B)	Continuous open	None	Moderate secondary carbonation	QMF - Mylonites Argentera - Mercantour		
AP_008	-	No	Yes	Yes	Impressa (PND1A)	Continuous closed	Instrumental	Secondary carbonation	QMF - Mylonites Argentera - Mercantour		
AP_011	-	Yes	Yes	No	Impressa (PND1A)	Continuous open	Digitо-ungual	Secondary carbonation	QMF - Mylonites Argentera - Mercantour		
AP_018	74P15 & hs	No	Yes	No	Impressa (PND1A)	Continuous closed	Instrumental	Secondary carbonation	QMF - Mylonites Argentera - Mercantour		
AP_028	-	Yes	Yes	No	Impressa (PND1B)	Discontinuous closed (neck)	None	Significant secondary carbonation; red dye	QMF - Mylonites Argentera - Mercantour		
AP_039	47856	No	Yes	Yes	Impressa (PND1B)	Continuous closed	Digitо-ungual	Moderate secondary carbonation	QMF - Mylonites Argentera - Mercantour		
AP_045	-	No	Yes	Yes	Impressa (PND1A)	Continuous closed	None	Secondary carbonation	QMF - Mylonites Argentera - Mercantour		
AP_049	Including one annealed sherd	No	No	No	Impressa (PND1A)	Discontinuous closed (neck)	Instrumental	Secondary carbonation	QMF - generic		
AP_070	4719	No	No	No	Impressa (PND1B)	Continuous, closed	Digitо-ungual	Secondary carbonation	QMF - generic		
AP_080	-	No	No	No	Impressa (PND1B)	Undefined	Digitо-ungual	Moderate secondary carbonation	QMF - generic		
AP_081	340015	No	No	No	Impressa (PND1A)	Undefined	Digitо-ungual	Moderate secondary carbonation	QMF - generic		
AP_091	25118	No	No	No	Cardial (PND2)	Undefined	None	Moderate secondary carbonation	QMF - generic		
AP_093	26693	No	No	No	Impressa (PND1B)	Undefined	Instrumental	Significant secondary carbonation	QMF - generic		
AP_094	hs	No	No	No	Impressa (PND1-indivise)	Undefined	Instrumental	Moderate secondary carbonation	QMF - generic		
AP_112	17850	No	No	No	Impressa (PND1A)	Undefined	Plastic	Moderate secondary carbonation	QMF - generic		
AP_177	Sherds A & B	No	Yes	No	Cardial (PND2)	Discontinuous closed (neck)	Cardiidae	Moderate secondary carbonation	QMF - Maures , Metamorphism		
AP_206	19302 & 42161	No	No	No	Cardial (PND2)	Undefined	Cardiidae	Moderate secondary carbonation	QMF - generic		

Table 1 – Main characteristics of the ceramics analysed in this study.
Tabl. 1 – Principales caractéristiques des céramiques analysées dans cette étude.

Chemical elements			Chemical elements taking into account in this study (n=22)
All the analyses (100 %) are > LOD	n = 7	Al, Si, P, K, Fe, Rb, Zr	
More than 95 % of the analyses > LOD	n = 13	Previous + S, Zn, Sr, Y, Nb, Ba	
More than 85 % of the analyses > LOD	n = 16	Previous + Ca, Pb, Th	
More than 75 % of the analyses > LOD	n = 18	Previous + Mn, Ni	
More than 50 % of the analyses > LOD	n = 22	Previous + Mg, Co, As, Sn	

Table 2 – Chemical elements analysed using the VANTA VMR portable XRF instrument (Olympus) with sufficient concentration in the samples (above the detection limit of the instrument, LOD).

Tabl. 2 – Eléments chimiques analysés à l'aide de l'appareil XRF portable VANTA VMR (Olympus) dont la concentration dans les échantillons est supérieure à la limite de détection (LOD) de l'appareil.

		QMF	GL	MIX	TOTAL
Impressa	Phase 1A	8	7	5	20
Impressa	Phase 1B	12	42	30	84
Cardial	Phase 2	5	43	6	54
		Total			158

QMF : Quartz-mica-feldspar group.

GL: Glauconitic marl and clay.

MIX: Mixed pastes.

The 17 ceramics studied in this study belong to QMF group (14 reported to Impressa, 3 to Cardial). Cf. table 1.

Table 3 – Distribution and total number of ceramics from the Pendimoun rock shelter.

Tabl. 3 – Répartition et nombre total de céramiques de l'abri Pendimoun.

two ferro-magnesian rich samples (Biotite, Ferriferous mica and Magnesian Phlogopite mica).

In a second step, in order to control matrix effects, twenty internal standards were analysed. These were weathering terreae sampled around the Argentera-Mercantour massif and foothills ($n = 8$), the Maures ($n = 4$) and Tanneron ($n = 5$) massifs and the Roc d'Orméa foothills ($n = 3$). These “terres d'intérêt” (TI), which constitute the potential sources of the studied ceramics (table 1), were the subject of experimental cooking at different temperatures, petrographic analyses and, for most of them, geochemical analyses by (major) ICP-AES and (trace) ICP-MS (SD.8; Gabriele *et al.*, this volume; Lardeaux *et al.*, this volume). For the present study, only the “terres d'intérêt” (TI) heated to 700°C were analysed using portable XRF and compared to the archaeological ceramics.

Each of the reference samples, CRM and TI, were analysed twice using the portable analyser. Supplementary data 7 and 8 (SD.6 and SD.7) give the percentage and/or ppm values for all the chemical elements included in this study. The seven analyses of the equatorial profile of AP-001 ceramic gave outliers for two elements Si and Al with respectively more than 345,000ppm and 140,000ppm, *i.e.* more than 75% and 27% of SiO_2 and Al_2O_3 , corresponding to outliers. We therefore did not take these values into account in the rest of the study.

RESULTS: ASSESSMENT OF ACCURACY AND REPEATABILITY

Measurement accuracy is the closeness of agreement between a measured value and a value considered to be true, or certified (JCGM, 2012). Repeatability can be equated with measurement precision, *i.e.* the closeness of agreement between measured values of the same object during repeated measurements (JCGM, 2012).

Elements detected by the analyser

In order to assess the accuracy of the measurements, it was necessary to work on chemical elements present in both the sample and the reference material as well as in sufficient quantities to be measured by the apparatus, *i.e.* whose concentration (or content) is higher than the limit of detection (LOD).

Thus, although the instrument used theoretically measures forty-one chemical elements using the “Geochem-REE-extra” mode, not all of them are present in sufficient quantity in the samples to be correctly measured by the portable analyser. Our study therefore only retains the chemical elements whose contents in the ceramic bodies studied are sufficient to be correctly measured, *i.e.* those whose measured content is higher than the LOD in at least 50% of the measurements ($n = 22$, table 2). For the other chemical elements theoretically measured by the analyser ($n = 20$), the levels measured in the samples are below the LOD in more than one analysis out of two.

Finally, within our ceramic corpus, the elements detected by the portable analyser are both “major” (Al, Si, K, Ca, Fe, P, Mg), “minor” (Mn) and “trace” elements (Ni, Rb, Zr, Sr, Y, Ba, Nb, Pb, Th, Co, Zn, Ni, As, Sn; table 2).

Accuracy of measurements

In our study, the accuracy of the handheld device is controlled with reference to the certified material (CRM) and the “terres d'intérêt” (TI) studied in the framework

of the CIMO programme (figs. 3 to 5). Table 4 shows the correlation coefficient (R^2) calculated using the expected values (certified values for CRMs and measured values in ICP-AES and ICP-MS for TIs) compared to the values measured with the portable XRF.

Accuracy of CRM measurements

Concerning the CRMs, the coefficient of correlation (R^2) values above 0.99 (Mg, Ca, Fe, Zn, Sr, Zr) and those between 0.92 and 0.99 (Si, P, K, Mn, Ni, Nb, Rb, Sn, Pb, Th and Ba) indicate a very good capacity of the analyser to measure these seventeen (17) elements in concentration ranges from several tens of per cent (Si) to a few ppm (Zr for example). For the lowest concentrations, the Zr concentration of the CRM "Mica Mg" for example is certified at 16ppm and the analyser measured 10 and 9ppm; or the Sr concentration of the CRM "Granite GH" is certified at 8.7ppm and the analyser gave 9 and 11ppm respectively for each of the two measurements carried out (fig. 3).

The correlation coefficient is lowest for yttrium ($R^2 = 0.784$) due to the difficulty of the pXRF to correctly measure the CRM "Mica-Fe" (fig. 3) certified at 48ppm whereas the portable analyser indicates values of 18 and 23ppm. When this CRM is not taken into account, the R^2 correlation coefficient rises to 0.994 for the Y.

Finally, the measurements are very poor ($R^2 < 0.586$) for three elements: Al, Pb and Co. For the first two, the R^2 correlation coefficient is much better when only TIs are taken into account (without CRMs), whereas for Co, the measurements made by the portable analyser are always far from the expected measurements, whether for CRMs or TIs.

The portable analyser measurements of all twenty-one chemical elements considered in this study were compared to reference values for three granitic CRMs (fig. 4). In order to be able to compare widely varying range of content, the data was normalised to the continental crust (Taylor and McLennan, 1995). This diagram provides an overview of the elements for which pXRF measurements allow reproducibility of certified measurements (Al, Si, K, Ca, Mn Fe, Rb, Sr, Y, Zr, Nb, Sn, Ba, Pb, Th).

Accuracy of TI measurements

The TI used as "internal standards" are raw materials fired at 700°C to approximate the ceramic pastes.

They present similar matrix effect to those of the analysed ceramics and thus allow to check the accuracy of the measurements. By limiting this matrix effect, we expected to obtain a better accuracy, *i.e.* closer proximity of the values measured with the analyser to the expected values. On the contrary, the measurements made with the portable XRF are further away from the expected measurements for eighteen of the twenty-one elements considered in our study (table 4).

For two elements (Al and Y), however, the TI measurements are closer to the expected values than for the CRMs. Thus, for aluminium, R^2 is 0.725 for TI (against 0.024 for CRM) and for Y, R^2 increases to 0.92 (against 0.78). For these two elements, a calibration using TIs could therefore bring a significant gain in the accuracy of the measurements of the portable device.

We do not have a simple explanation for these observations. However, they underline that matrix effects have, for some chemical elements, a real influence on the automatic deconvolution of X-ray spectra.

Repeatability of the measurements

In order to test the repeatability of the measurements, each CRM was measured twice with the portable analyser. The mean and standard deviation of these measurements (table 5; fig. 5) indicate a good stability of the analyser and therefore correct repeatability of the measurements in the content ranges represented by the CRMs. Table 5 shows that the standard deviations of the measurements are often less than 5% of the measured value for the twenty-one elements of the six CRMs analysed. It would obviously be necessary to multiply these measurements over a longer period of time in order to control the repeatability of the apparatus even more precisely and to check the possible analytical drifts over several months.

RESULTS AND DISCUSSION

The results presented here show both good repeatability -which should be confirmed in a more systematic way in later studies- and good accuracy for several chemical elements present in the ceramic bodies.

NAME	Mg	Al	Si	P	S	K	Ca	Mn	Fe	Co	Ni	Zn	As	Rb	Sr	Y	Zr	Nb	Sn	Pb	Th	Ba
R2 (CRM)	0,995	0,024	0,958	0,960	NA	0,950	0,999	0,949	0,993	0,068	0,967	0,997	NA	0,982	1,000	0,784	0,992	0,978	0,935	0,924	0,974	0,980
R2 (TI)	0,977	0,725	0,671	0,795	NA	0,769	0,963	0,644	0,976	0,003	0,944	0,904	0,000	0,856	0,975	0,918	0,927	0,846	0,013	0,709	0,644	0,920
R2 (CRM & TI)	0,980	0,567	0,697	0,774	NA	0,896	0,965	0,883	0,980	0,035	0,954	0,990	0,004	0,981	0,998	0,840	0,979	0,982	0,678	0,704	0,972	0,980

In bold, $R^2 > 0,92$. Normal: $0,71 > R^2 > 0,92$. Red: $R^2 < 0,6$

For S and As, the absence of a certified value does not allow the calculation of R^2 .

Table 4 – Correlation coefficients (R^2) between the "certified" values and the values "measured" using a portable XRF for twenty-one elements of the CRM and TI heated to 700°C.

Tabl. 4 – Coefficients de corrélation (R^2) entre les valeurs « certifiées » et « mesurées » par le XRF portable pour vingt-et-un éléments des CRM et des TI chauffées à 700°C.

NAME	NBR ANAL	Mg (%)	Al (%)	Si (%)	P (%)	K (%)	Ca (%)	Mn (%)	Fe (%)	Co (%)	Ni (%)	Zn (%)	
		(σ %)	(σ %)	(σ %)	(σ %)	(σ %)	(σ %)	(σ %)	(σ %)	(σ %)	(σ %)	(σ %)	
Basalt_BR	2	67 848	51 129	164 578	5 091	9 929	98 758	1 334	85 174	511	379	220	
		167 (0.25)	404 (0.79)	723 (0.44)	24 (0.47)	63 (0.63)	272 (0.28)	81 (6.10)	37 (0.04)	135 (26.46)	45 (11.94)	6 (2.90)	
Granite_GA	2	7 409	70 201	318 200	637	34 137	19 101	943	21 264	147	< LOD	118	
		173 (2.33)	389 (0.55)	120 (18.77)	484 (1.42)	369 (1.93)	4 (0.45)	197 (0.93)	1 (0.96)	-	-	4 (3.01)	
Granite_GH	2	< LOD	93 416	350 530	183	41 826	5 145	519	11 383	< LOD	< LOD	103	
		-	43 338 (47.03)	17 498 (4.99)	20 (10.82)	1 385 (3.31)	56 (1.09)	230 (40.50)	536 (4.71)	-	-	4 (3.45)	
Granite_GS_N	2	9 090	55 584	254 871	1 145	34 693	17 251	< LOD	25 828	172	< LOD	52	
		973 (10.70)	1 530 (2.75)	5 189 (2.04)	29 (2.53)	135 (0.39)	62 (0.36)	< LOD	-	199 (0.77)	19 (11.13)	-	
Granite_Fe	2	22 675	71 532	124 529	1 320	56 447	722	2 194	145 379	669	< LOD	1 242	
		354 (1.56)	1 006 (1.40)	1 249 (1.00)	1 (0.05)	210 (0.37)	42 (5.78)	33 (1.48)	797 (0.55)	146 (21.90)	-	3 (0.23)	
Mica_Mg	2	114 069	65 604	166 682	113	78 123	< LOD	1 986	63 293	259	131	347	
		1 693 (1.48)	100 (0.15)	316 (0.19)	20 (17.52)	321 (0.41)	-	29 (1.46)	747 (1.18)	70 (27.08)	1 (0.54)	24 (6.93)	
NAME	NBR ANAL	Rb (%)	(σ %)	Sr (%)	(σ %)	Y (%)	(σ %)	Zr (%)	(σ %)	Nb (%)	(σ %)	Sn (%)	(σ %)
		(σ %)	(σ %)	(σ %)	(σ %)	(σ %)	(σ %)	(σ %)	(σ %)	(σ %)	(σ %)	(σ %)	(σ %)
Basalt_BR	2	41	1 310	27	240	103	17	< LOD	< LOD	< LOD	< LOD	1 090	
		1 (3.45)	8 (0.59)	1 (2.67)	1 (0.59)	1 (1.37)	1 (4.29)	-	-	-	-	-	6 (0.58)
Granite_GA	2	175	327	22	138	13	< LOD	37	19	16	19	1 131	
		7 (4.04)	9 (2.82)	2 (9.87)	14 (10.25)	- (0.00)	-	3 (7.64)	1 (7.44)	4 (22.81)	4 (0.31)	-	-
Granite_GH	2	401	10	83	162	98	< LOD	42	91	19	< LOD	1 671	
		26 (6.53)	1 (14.14)	1 (0.86)	13 (8.32)	- (0.00)	-	8 (18.74)	11 (12.43)	6 (29.77)	-	-	-
Granite_GS_N	2	173	576	13	213	22	< LOD	48	38	< LOD	< LOD	1 671	
		8 (4.51)	3 (0.49)	1 (5.66)	1 (0.33)	1 (6.43)	-	1 (2.95)	(0.00)	-	-	15 (0.89)	
Mica_Fe	2	1 555	< LOD	21	625	223	63	< LOD	122	57	76	76	
		1 (0.05)	-	4 (17.25)	4 (0.68)	1 (0.63)	- (0.00)	-	13 (10.43)	3 (4.96)	4 (5.58)	-	
Mica_Mg	2	1 143	26	< LOD	10	114	< LOD	< LOD	< LOD	3 728	3 728	-	
		- (0.00)	3 (10.88)	-	1 (7.44)	1 (0.62)	-	-	-	-	-	75 (2.01)	

Table 5 – Means (in bold) and standard deviations of CRM measurements made using a VANTA portable XRF. For each element, the right column shows the percentage of the standard deviation compared to the mean. Observe the low standard deviation for most of the elements measured.

Table 5 – Moyennes (en gras) et écarts-types des mesures des CRM réalisées à l'aide du XRF portable VANTA. Pour chaque élément, la colonne de droite indique le pourcentage de l'écart-type par rapport à la moyenne (en %). Observer la faiblesse de l'écart-type pour la plupart des éléments mesurés.

In this context, the following discussion focuses on three points identified at the start of this study. Firstly, the extent to which the portable analyser is able to differentiate between the sources (TI) used in the manufacture of the ceramics. Then, we question the capacity of the analyser to correctly attribute a sherd to one of the potential sources (TI). Finally, we discuss the possibility of evaluating the heterogeneity of the pastes used for making some of the pots and the possibility to detect taphonomic effects that could disturb the geochemical signal.

Characterising the “*terres d’intérêt*”

The sourcing carried out during the CIMO programme, based on petrographic, microstructural and geochemical analyses, has enabled to identify three potential sources of terrae for the Pendimoun rock shelter ceramic pastes: first, terrae from the alteration of Argentera-Mercantour mylonites; second, terrae deposits associated with the Maures-Tanneron metamorphic rocks; and third, sedimentary marls and terrae of Cretaceous origin from the Roc d'Orméa foothills (Gabriele *et al.*, this volume; Lardeaux *et al.*, this volume).

The new analyses carried out in the present study aim to assess the extent to which the portable XRF analyser can recover these distinctions. The SiO_2 vs Al_2O_3 binary diagram allows to partially distinguish these sources, grouped on three different clusters on the figure 6. Among these sources, the Argentera-Mercantour mylonite alteration materials have the highest SiO_2 content (>50%). The terrae from the alteration of the metamorphic rocks of the two Maures and Tanneron massifs come from the same geological, petrographic and structural group (Toutin-Morin *et al.*, 1994) and are characterised, in both cases, by Al_2O_3 contents ranging between 15 and 27%. Finally, the soils of the Orm a foothills are clearly distinguished from the other plutonic or metamorphic TI by lower values of SiO_2 (< 43%) and Al_2O_3 (< 7.5%).

Other plots as $\text{SiO}_2/\text{Al}_2\text{O}_3$ vs Fe_2O_3 (SD. 9) show similar information without completely removing some overlap between the geochemical domains of the three main sources. The multi-element diagram (SD. 10) representing some of the chemical elements allows us to identify the most discriminating elements: mainly CaO , Nb , and Zr .

Finally, the diagram of the twenty-one chemical elements normalized to the continental crust (SD. 11) allows an overall visualization. Despite the continuity of the measured values for most chemical elements, these TIs can be partially distinguished, notably those of the Argentera with low Ca contents and those of the Ormeá with low Al or Zr values.

It thus appears that the portable X-ray fluorescence device allows a suitable separation of the potential sources ("TI"). However, our data show how essential it is to associate XRF analyses with mineralogy and petrography. Finally, it seems illusory to claim that portable XRF may be able to distinguish "sub-sources" within the three main sources ("TI").

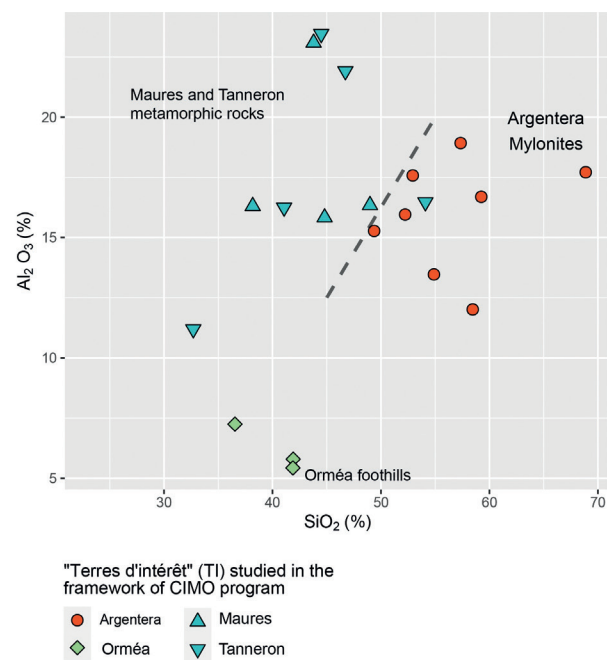


Fig. 6 – SiO_2 vs. Al_2O_3 diagram showing portable XRF analyses of the 20 TI heated to 700°C. This graph is completed by SD.9 (the $\text{SiO}_2/\text{Al}_2\text{O}_3$ vs Fe_2O_3 diagram), SD.10 (multi-element diagrams) and SD.11 (concentrations normalized to the continental crust).

Fig. 6 – Diagramme SiO_2 vs. Al_2O_3 montrant les analyses XRF-portables des 20 terres d'intérêt (TI) cuites à 700°C. Ce graphique est complété par les DS.9 (le diagramme $\text{SiO}_2/\text{Al}_2\text{O}_3$ vs Fe_2O_3), DS.10 (diagrammes multi-élémentaires) et DS.11 (concentrations normalisées à la croûte continentale).

Attributing a ceramic to a source (TI)

In order to identify the potential sources of the studied ceramics, their compositions were compared with those of the geological references (TI) using the most discriminating elements. Their position on the SiO_2 vs. Al_2O_3 diagram (fig. 7 and fig. 8; SD.9 and SD.10) indicates the Argentera-Mercantour as the probable origin of the pastes for most ($n = 15$) of the twenty-one sherds belonging to the seventeen studied ceramics. The portable XRF analyses are therefore consistent with the mineralogical, petrographical and geochemical results previously obtained in the framework of the CIMO programme (table 1).

On the basis of figure 7 alone, sherds AP028, AP08, AP093, AP045, AP11 and AP049 are difficult to attribute. They are indeed in an intermediate position between the different sources ("TI"), with relatively low SiO_2 and Al_2O_3 values. This situation is probably linked to the high CaO values (> 7%) consistent with the secondary carbonations observed on all these sherds (table 1) and which lead, in this figure, to the exclusion of these sherds from the Argentera-Mercantour Mylonite group. These higher CaO content slightly modify the relative value of other major elements (table 1).

The ternary plot Fe_2O_3 , Al_2O_3 , SiO_2 (fig. 8) allows to better distinguish the three sources ("TI"). The terrae sources located around the Piedmont of Ormeá present

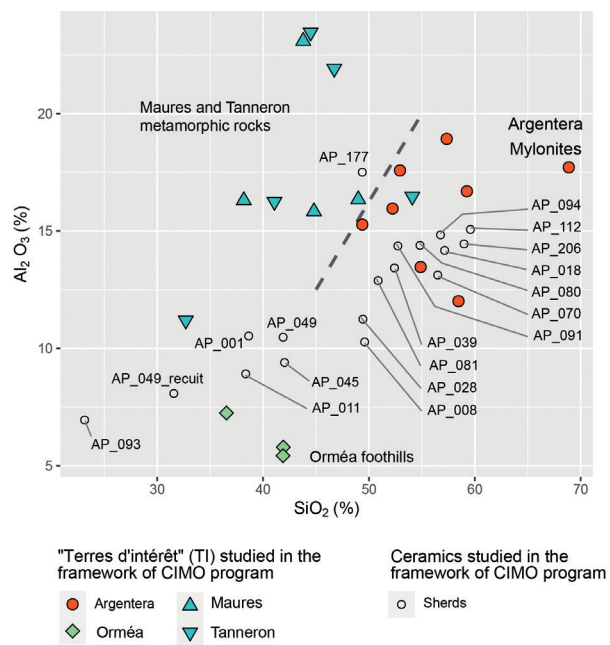


Fig. 7 – Position of the twenty-one shards (belonging to the seventeen studied ceramics) on the SiO_2 vs. Al_2O_3 diagram, compared with the potential sources heated at 700°C

Fig. 7 – Position des vingt-et-un tessons (appartenant à dix-sept céramiques) sur le diagramme SiO_2 vs. Al_2O_3 comparée avec les sources potentielles (terres d'intérêt) chauffées à 700°C.

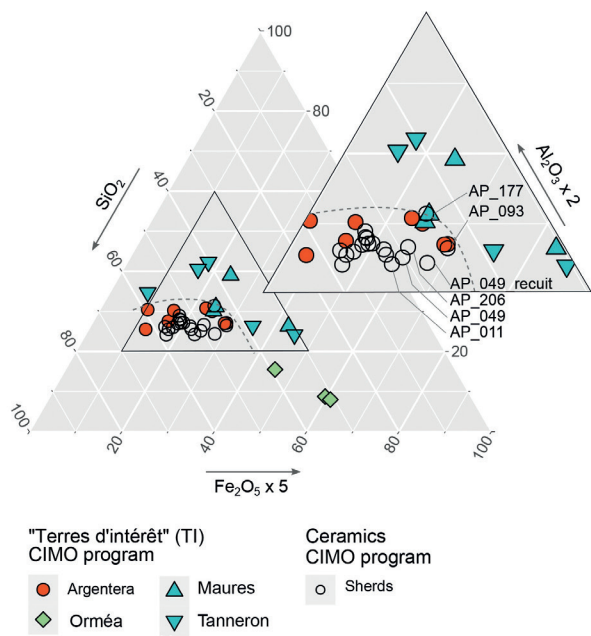


Fig. 8 – Position of the twenty-one shards (belonging to the seventeen ceramics) on a ternary diagram Fe_2O_3 , Al_2O_3 , SiO_2 (%). In order to better separate the groups, the Fe_2O_3 and Al_2O_3 contents have been multiplied by 5 and 2 respectively.

Fig. 8 – Position des vingt-et-un tessons (appartenant aux dix-sept céramiques) sur un diagramme ternaire Fe_2O_3 , Al_2O_3 , SiO_2 (%). Afin de mieux séparer les groupes, les teneurs en Fe_2O_3 et Al_2O_3 ont été multipliées, respectivement par 5 et 2.

relatively higher values of Fe_2O_3 compared to the two other sources. In this figure 8, the sherds are correctly grouped around the Argentera-Mercantour TI. On this plot, only two ceramics (AP177 and AP093) are in an intermediate position where the TI are difficult to differentiate.

Figure 8 shows that AP177 ceramic has SiO_2 (49.4%), Al_2O_3 (17.5%) and Fe_2O_3 (5.42%) contents for which there is confusion between the Maures-Tanneron and Argentera sources. This situation can be associated with the carbonate deposit, well measured by the portable analyser which indicates a higher CaO content (8.75%) than the other sherds. Previous observations of the thin section had attributed AP177 to the Maures metamorphism (table 1).

In figure 8 sherd AP093 occupies a similar location on the plot where the Maures-Tanneron and Argentera sources overlap. Mesoscopic observation had previously assigned this sherd to the QMF group (table 1) and did not show any inclusions that could suggest a mixing with glauconitic materials. In thin section, AP093 present numerous microclines minerals, but they have not altered the chemical measurements: the K_2O content (2.65%) is in comparable ranges to the other sherds. However, once again, the important carbonate deposit, partly invading the decorative impressions, was well measured by the portable analyser (13.3% CaO) and played a role in the relative concentrations of major elements.

These observations show the importance of the taphonomic processes that we discuss in the next section.

Heterogeneities and/or taphonomic process: possible effects on the p-XRF measurements

Recent research has demonstrated and documented the manufacture of ceramics from the Impressa and Cardial horizons of Pendimoun by the Spiralled Patchwork technique (SPT, Gomart *et al.*, 2017; Gomart, Binder, Gabriele *et al.*, this volume). Furthermore, the mixing of terreae of different origins was observed recurrently in the same ceramic, forming mixed pastes (MIX). They present the joint presence of minerals or rock fragments entering in the composition of glauconitic pastes (GL) and "granitic" pastes (QMF). These two independent technical characteristics (*i.e.* the assembly by juxtaposition of small spiral elements and the potential use of different earths for the assembly of the same ceramics) clearly pose the hypothesis of a strong variability of chemical compositions within certain ceramics.

In order to test this last hypothesis, longitudinal and equatorial transects were carried out for two particularly well-preserved ceramics from the QMF group (AP001 and AP045) (fig. 9). Sixteen and twenty-two measurements were made on each of these ceramics respectively. For AP001, the results do not reveal any significant spatial geochemical heterogeneity, suggesting that this ceramic was built with a unique source of materials originated from the Argentera-Mercantour massif.

On the other hand, for the AP045 ceramic, the transect shows a strong variability of three main elements,

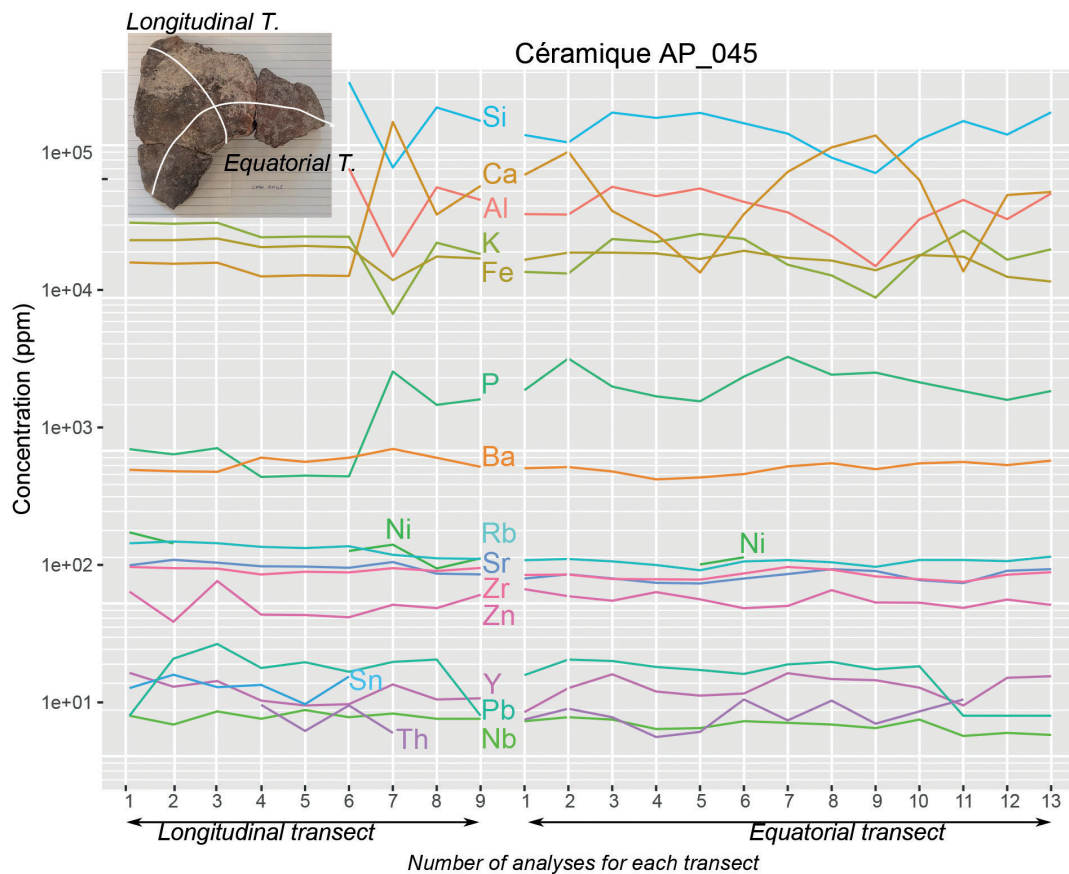
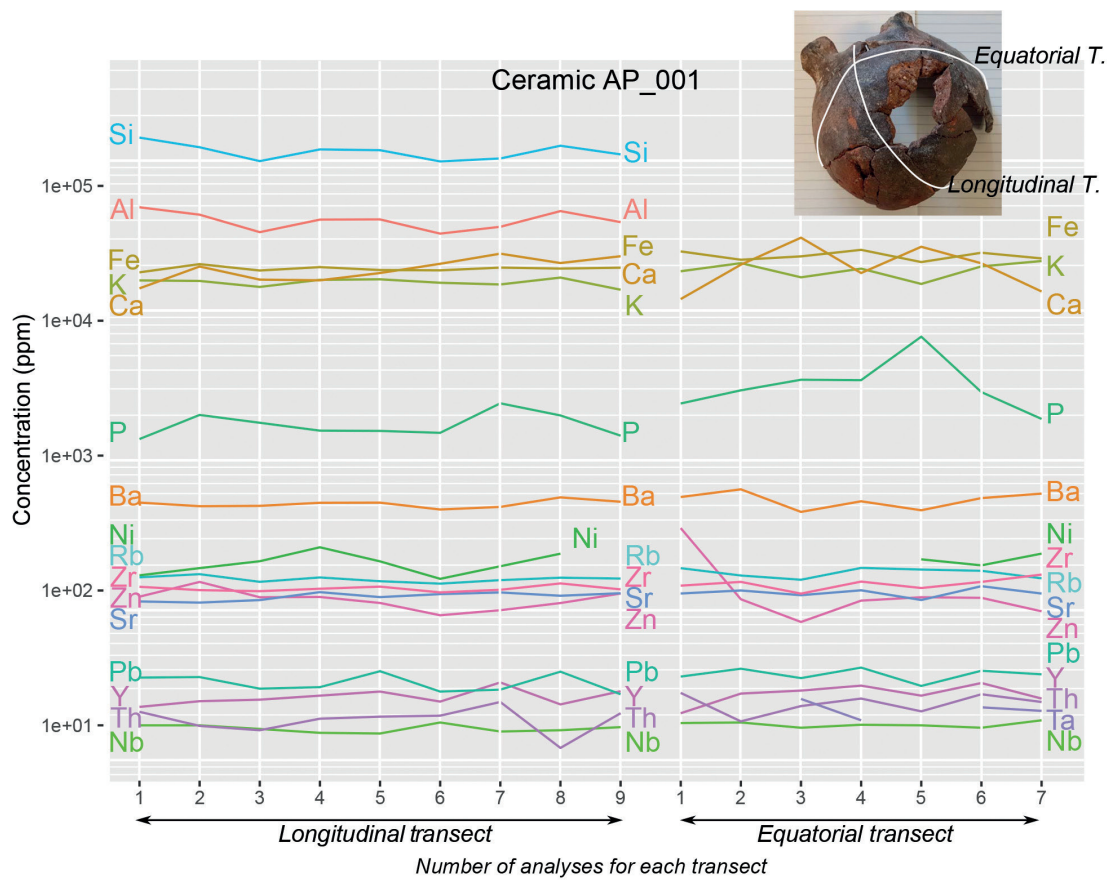


Fig. 9 – Analyses (portable XRF) carried out along the longitudinal and equatorial transects, through the ceramics AP001 and AP045.
Fig. 9 – Résultats des analyses XRF-portable réalisées selon les transects longitudinaux et équatoriaux, à travers les céramiques AP001 et AP045.

calcium (Ca), phosphorus (P) and potassium (K). This variability can be attributed to a taphonomic effect rather than to a real heterogeneity of the pastes. Indeed, calcium is particularly mobile and abundant in an open rock shelter context in limestones. Phosphorus is an element associated with organic matter and human occupation of the rock shelter. The variation in K content could be related to its relative mobility under weathering conditions. We also hypothesis that it could also be due to the random density of potassium feldspar phenocrysts under the measurement spot -even if this hypothesis was rejected in in the case of ceramic AP093 (see above).

The thin (sub-millimetre) superficial deposits overlying the archaeological material are not able to alter the results of an XRF analysis. Indeed, the X-ray penetrates the material to depths of a few millimetres, greater than the thickness of most crusts (Liritzis and Zacharias, 2011). However, in some cases, the thickness of the crusts or the porosity of the pastes could be at the origin of a redistribution of the elements within a higher thickness of the sherd. Thus, we have seen that, among the sherds studied, AP093 and AP011 show carbonate crusts clearly visible to the naked eye and XRF analysis revealed high CaO contents of 13.3 and 16.5% respectively.

The estimation of the porosity of the Pendimoun vases built from granitic soils provides some keys to interpret these data. Indeed, analysis by mercury intrusion porosimetry (Drieu *et al.*, 2019) indicates that unlike glauconitic pastes, those derived from mylonite alteration are characterised by the absence of very small pores ($< 0.1\mu\text{m}$), with a very strong dominance of large pores (between 1 and $50\mu\text{m}$). This very open porosity may favour the pollution of the shards by mobile elements resulting either from the dissolution of carbonates from the rock face, or from the redistribution of organic juices linked to the use of the shelter as a sheepfold.

Another taphonomic evolution may be linked to repeated firing phenomena after the vases were abandoned. Thus, sherds AP049 (fired) and AP018 (74P15) were fired after the vases were fragmented. Analyses of the fired sherds show chemical variations compared to analyses of the unfired sherds coming from the same pots (SD. 12). For AP049, a decrease in SiO_2 content (41.9 to 31.6%) and secondarily in Al_2O_3 (10.5 to 8.1%) is observed, mainly in favour of CaO (6.5 to 14.5%). However, the evolution is the opposite for AP018 with a relative enrichment in SiO_2 and Al_2O_3 and a depletion in CaO.

CONCLUSIONS

The quality of geochemical measurements (accuracy, repeatability) made with portable X-ray fluorescence equipment depends on several factors. Firstly, the instrument itself (*e.g.* sensitivity of the sensors, more or less efficient algorithms for interpreting or “deconvoluting” the complex spectra) must be taken into account. The nature of the samples also plays a major role in the quality

of the measurements, whether it be the heterogeneity of the materials (granulometry, mineralogy, water content, porosity, etc.) or matrix effects. Finally, as with any measurement, the analytical protocol is essential: in particular, it must be based on the use of international (CRM) and/or internal standards (in-house standards) which allow the accuracy and repeatability of measurements to be controlled.

Once these elements have been taken into account, the data discussed here show the reliability of the measurements carried out using the portable X-ray fluorescence analyser. Indeed, the latter shows an excellent capacity to reproduce the expected measurements on certified materials (CRM). This very good precision was also verified on the “terres d’intérêt” (TI) that had previously been the subject of petrographic characterization as well as chemical analyses by ICP-AES and ICP-MS and whose matrices are close to those of the ceramics that we wished to characterise.

The correlations between the expected measurements (certified or reference) and those carried out with the portable analyser on CRMs and TIs show that the analyser reproduces the expected measurements of CRMs with greater precision. It can be assumed that the lower accuracy obtained for TIs is partly related to their composition, which is more heterogeneous than that of the international standards. For this study, the accuracy associated with the “factory” calibration was found to be sufficient to allow the analyser to distinguish between the different sources (“TI”), without the need to calibrate the instrument. In this case, the use of CRMs and in-house standards allows this accuracy to be controlled. For further studies on other materials, however, it may be necessary to calibrate the analyser.

The TIs resulting from the alteration of the Argentera-Mercantour mylonites form a coherent group that is very different from the marls and clayey formations from the Ormea foothills and from the terrae outcropping in and around the Maures-Tanneron massif. Nevertheless, this last geological ensemble does not define a restricted geochemical domain: the characteristics of the Maures-Tanneron materials remain dispersed.

In these conditions, the p-XRF analyses easily allow us to differentiate the ceramics (fig. 7 and fig. 8) whose raw material comes from the Argentera-Mercantour which constituted the essential part of the analysed corpus (15/17) and the ceramic (AP177) using paste whose chemical characteristics are within the variability of those of the Maures-Tanneron. Concerning the ceramic AP093, if it is not a resource not yet identified, the particular composition could indicate an important pollution linked to deposits after its abandonment.

The analyses carried out for this study did not allow us to observe any internal variability likely to argue for a mixture of pastes. The mesoscopic observations are therefore, from this point of view, generally conclusive. The variability in chemical composition observed on the two transects seems to be generated by the burial conditions of the ceramic remains, which can be observed

macroscopically. Therefore, the chemical elements likely to be linked to differential burial conditions and water circulation (Ca, P, K) must be used with caution to characterise the pastes and establish their origin.

Two methodological points deserve particular attention. Firstly, this assessment shows the importance of prior knowledge of potential sources in terms not only of geochemistry but also of petrography and mineralogy. The field and laboratory knowledge enables the quality and credibility of the analyses to be verified. Secondly, it is absolutely necessary to carry out, in parallel with any set of portable XRF analyses, repeated measurements of certified materials and internal standards, which are the only way to check the robustness of the analyses.

Finally, this study demonstrates that, when associated with a naturalistic approach providing a prior knowledge of petrographic and geochemical of the potential sources, the use of the portable XRF makes it possible to carry out non-destructive studies on a large number of ceramics in a relatively constrained period of time and to distinguish the main sources quickly and efficiently.

LIST OF SUPPLEMENTARY INFORMATION AND DATA / LISTE DES INFORMATIONS ET DONNÉES SUPPLÉMENTAIRES

SD-1 – Description of sampling contexts / *Description des contextes échantillonnés.*

SD-2 – Location of “granitic” alteration earths sampled in the Argentera-Mercantour massif and piedmont (geological map 1/50 000, BRGM, sheet n°1579) / *Les « Terres d’intérêt » de l’Argentera. Localisation des terres d’altération « granitiques » échantillonnées dans le massif et le piémont de l’Argentera-Mercantour (carte géologique 1/50 000 vecteur harmonisé, BRGM, Feuille N°1579).*

SD-3 – Location of “granitic” alteration earths sampled in the Maures massif (geological map 1/50 000, BRGM, sheet n°1359) / *Les « Terres d’intérêts » du massif des Maures. Localisation des terres d’altération « granitiques » échantillonnées dans le massif des Maures (carte géologique 1/50 000 vecteur harmonisé, BRGM, Feuille N°1359).*

SD-4 – Location of glauconitic marls and earths sampled in the Ormée piedmont (geological map 1/50 000, BRGM, sheet n°1579) / *Les « Terres d’intérêt » du piémont de l’Ormée. Localisation des marnes et terres glauconieuses échantillonnées dans le massif de l’Ormée (carte géologique 1/50000vecteurharmonisé, BRGM, Feuille N°1579).*

SD-5 – Location of “granitic” alteration earths sampled in the Tanneron massif (geological map 1/50 000, BRGM, sheet n°1359) / *Les « Terres d’intérêts » du massif du Tanneron. Localisation des terres d’altération « granitiques » échantillonnées dans le massif du Tanneron (carte géologique 1/50 000 vecteur harmonisé, BRGM, Feuille N°1359).*

SD-6 – Portable XRF analyses of CRMs, TIs heated to 700°C and ceramics from the CIMO program, processed during the two sessions in February and July 2019 / *Analyses à l’aide du XRF-portable des CRM, des TI chauffées à 700°C et des céramiques du programme CIMO, réalisées lors des deux sessions de février et juillet 2019.*

SD-7 – Means and standard deviations of portable XRF analyses of CRMs and CIMO ceramics (February and July 2019) / *Moyennes et écarts type des analyses des réalisées à l’aide de l’analyseur XRF portable des CRM et des céramiques du programme CIMO (février et juillet 2019).*

SD-8 – Elements identified by ICP-AES and ICP-MS in geological reference samples (raw and experimentally fired) and archaeological samples / *Table des éléments identifiés par ICP-AES et ICP-MS dans les échantillons de référence géologiques (crus et cuits expérimentalement) et des échantillons archéologiques.*

SD-9 – $\text{SiO}_2/\text{Al}_2\text{O}_3$ vs Fe_2O_3 diagram allowing to distinguish the terrae coming from the Col de l’Orme, without removing the existing confusions between the three other “terrae of interest” (cf. figure 4) / *Diagramme $\text{SiO}_2/\text{Al}_2\text{O}_3$ vs Fe_2O_3 permettant de distinguer les terres provenant du col de l’Orme, sans pour autant supprimer les confusions existantes entre les trois autres « terres d’intérêt » (cf. figure 4).*

SD-10 – Harker diagram for some chemical elements allowing to characterise the “terrae of interest” of the CIMO program. The SiO_2 vs. CaO or Zr vs. Nb diagrams are the most discriminating in addition to the SiO_2 vs. Al_2O_3 diagram (figure 4A) / *Diagramme de Harker pour quelques éléments chimiques permettant de caractériser les « terres d’intérêt » du programme CIMO. Les diagrammes SiO_2 vs. CaO ou Zr vs. Nb sont les plus discriminants en plus du diagramme SiO_2 vs. Al_2O_3 (figure 4A).*

SD-11 – Chemical elements normalized to the continental crust. Some elements (Al, Ca, Nb, Zr) appear to be discriminating, but the figure highlights the difficulty in distinguishing between the different “terrae of interest”, visible in figure 4 or in SD.3 and 4 / *Éléments chimiques normalisés à la croûte continentale. Quelques éléments (Al, Ca, Nb, Zr) apparaissent discriminants, mais la figure souligne la difficulté à distinguer les différentes « terres d’intérêt », visible sur la figure 4 ou les DS.3 et 4.*

SD-12 – Variation of SiO_2 and Al_2O_3 concentration of fired shards compared to the same non-fired shards (samples AP_018 and AP_049) / *Variation de concentration en SiO_2 et Al_2O_3 de tessons recuits par rapport aux même tessons non recuits (échantillons AP_018 et AP_049). <https://doi.org/10.34847/nkl.a32ax334>*

Acknowledgements

This research was conducted as part of the CIMO project (ANR-14-CE31-009, under the direction of Didier

Binder, CNRS, Nice), which co-financed the acquisition of a pXRF by the GEOAZUR laboratory, a project partner.

Damase Mouralis, Didier Binder, Gilles Durrenmath and Chrystèle Verati carried out the pXRF measurements of the reference and archaeological samples. Damase Mouralis processed the data sets and wrote the article with

contributions from Didier Binder, Gilles Durrenmath, Jean-Marc Lardeaux and Chrystèle Verati. All co-authors reviewed the article and approved its content.

The authors would like to thank Guillaume Duclaux (GEOAZUR) for his advice on the implementation of the analyses.

REFERENCES

- BASSO E., BINDER D., MESSIGA B., RICCARDI M. (2006) – The Neolithic Pottery of Abri Pendimoun (Castellar, France): a Petro-Archaeometric Study. London, Geological Society (Special Publications, 257), p. 33-48.
- BELFIORE C. M., LA RUSSA M. F., BARCA D., GALLI G., PEZZINO A., RUFFOLO S. A., VICCARO M., FICHERA G. V. (2014) – A Trace Element Study for the Provenance Attribution of Ceramic Artefacts: the Case of Dressel 1 Amphorae from a Late-Republican Ship, *Journal of Archaeological Science*, 43, p. 91-104.
- BINDER D., LARDEAUX J.-M., MUNTONI I. M., DUBAR M., DURRENMATH G., JACOMET S., MONGE G., LEPÈRE C. (2018) – South-Eastern Italian Transfers Towards the Alps During the 5th Millennium cal BCE: Evidence of “Serra-d’Alto” Ware Within Square-Mouthed Pottery Deposits at the Lare 2 Cave (Saint-Benoit, Alpes-de-Haute-Provence, France), *Journal of Archaeological Science: Reports*, 21, p. 222-237.
- DRIEU L., HORGNIES M., BINDER D., PÉTREQUIN P., PÉTREQUIN A.-M., PECHÉ-QUILICHINI K., LACHENAL T., REGERT M. (2019) – Influence of Porosity on Lipid Preservation in the Wall of Archaeological Pottery, *Archaeometry*, 61, 5, p. 1081-1096.
- ERAMO G., MUNTONI I. M., GALLO S., DE SIENA A. (2018) – Approaching the Early Greek Colonization in Southern Italy: Ceramic Local Production and Imports in the Siritis *Journal of Archaeological Science: Reports*, 21, p. 995-1008.
- FORSTER N., GRAVE P. (2012) – Non-Destructive PXRF Analysis of Museum-Curated Obsidian from the Near East, *Journal of Archaeological Science*, 39, p. 728-736.
- FRAHM E. (2013) – Validity of “Off-the-Shelf” Handheld Portable XRF for Sourcing Near Eastern Obsidian Chip Debris, *Journal of Archaeological Science*, 40, p. 1080-1092.
- FRAHM E., CAROLUS C. M., CAMERON A., BERNER J., BROWN H., CHENG J., KALODNER J., LEGGETT J. L., NATALE A., SEIBERT S., SPARKS-STOKES D., WUELLNER E. (2022) – Introducing the BRICC (Bricks and Rocks for Instruments’ Ceramic Calibration) Sets: Open-Source Calibration Materials for Quantitative X-Ray Fluorescence Analysis. *Journal of Archaeological Science: Reports*, 43, p. 103443.
- GABRIELE M. (2014) – *La circolazione delle ceramiche del Neolitico nel medio e alto Tirreno e nell’area ligure-provenzale. Studi di provenienza // La circulation des céramiques néolithiques dans l’aire tyrrhénienne et dans l’aire liguro-provençale. Étude de provenance*, doctoral thesis, Università di Pisa and Université Nice – Sophia Antipolis, 437 p.
- GABRIELE M., VERATI C., CONVERTINI F., GRATUZE B., JACOMET S., BOSCHIAN G., DURRENMATH G., GUILAINE J., LARDEAUX J.M., GOMART L., MANEN C., BINDER D. (2019) – Long-Distance Mobility in the North-Western Mediterranean During the Neolithic Transition Using High Resolution Pottery Sourcing, *Journal of Archaeological Science Reports*, 29, p. 102050.
- GOMART L., WEINER A., GABRIELE M., DURRENMATH G., SORIN S., ANGELI L., COLOMBO M., FABBRI C., MAGGI R., PANELLI C., PISANI D., RADÍ G., TOZZI C., BINDER D. (2017) – Spiralled Patchwork in Pottery Manufacture and the Introduction of Farming to Southern Europe, *Antiquity*, 91, 360, p. 1501–1514.
- HUNT A. M. W., SPEAKMAN R. J. (2015) – Portable XRF Analysis of Archaeological Sediments and Ceramics, *Journal of Archaeological Science*, 53, p. 626-638.
- JCGM (2012) – *International Vocabulary of Metrology – Basic and General Concepts and Associated Terms (VIM)*, 3rd Edition 2008 Version with Minor Corrections Joint Committee for Guides in Metrology.
- LAVIANO R., MUNTONI I. M. (2006) – Provenance and Technology of Apulian Neolithic Pottery, in M. Maggetti and B. Messiga (eds.), *Geomaterials in Cultural Heritage*, London, Geological Society, p. 49-62.
- LAVIANO R., MUNTONI I. M. (2007) – Analisi archeometriche sulle ceramiche a figure rosse dalla tomba 33 di Timmari: provenienza delle materie prime e tecnologie di manifattura di alcune opere del Pittore di Dario, in M. G. Canosa (ed.), *Una tomba principesca da Timmari*, Rome, Giorgio Bretschneider, p. 189-205.
- LIRITZIS I., ZACHARIAS N. (2011) – Portable XRF of Archaeological Artifacts: Current Research, Potentials and Limitations, in M. S. Shackley (ed.), *X-Ray Fluorescence Spectrometry (XRF) in Geoarchaeology*, New York, Springer p. 109-142.
- MAGGETTI M. (1981) – Composition of Roman Pottery from Lousonna (Switzerland), in M. J. Hughes (ed.), *Scientific Studies in Ancient Ceramics*, London, British Museum Research Laboratory (British Museum Occasional Papers, 19), p. 33-49.
- MAGGETTI M. (1986) – Majolika aus Mexiko: ein archäometrisches Fallbeispiel, *Fortschritte der Mineralogie*, 64, 1, p. 87-103.

MOURALIS D. (2016) – *Apports de la géographie à l'étude des sources d'obsidienne d'Anatolie orientale : du terrain aux modèles*, HDR thesis, Université Paris 1 – Panthéon-Sorbonne), 216 p.

MUNTONI I. M., ERAMO G. (2016) – Archaeometric Analyses of Ceramic Materials, in E. S. Elster, E. Isetti, J. E. Robb, and A. Traverso (eds.), *The Archaeology of Grotta Scaloria: Ritual in Neolithic Southeast Italy*, Los Angeles, UCLA Cotsen Institute of Archaeology Press (Monumenta Archaeologica, 38), p. 253–265.

MUNTONI I. M., LAVIANO R. (2008) – Archaeometric Data on Production and Circulation of Neolithic Serra d'Alto Ware in Southern Italy During the Fifth Millennium BC, *ArcheoSciences, Revue d'Archéométrie*, 32, p. 125-135.

PICON M., LE MIÈRE M. (2002) – Géochimie des céramiques, in J.C. Miskovsky (ed.), *Géologie de la Préhistoire : méthodes, techniques, applications*, Paris, Association pour l'étude de l'environnement de la Préhistoire, p. 1001-1014.

SHACKLEY M. S. (2011) – An Introduction to X-Ray Fluorescence (XRF) Analysis in Archaeology, in M. S. Shackley (ed.), *X-Ray Fluorescence Spectrometry (XRF) in Geoarchaeology*, New York, Springer, p. 7-44.

SCHMITT A., CANTIN N., THIRION-MERLE V. (2009) – De la géochimie des productions provençales à pâte calcaire au référentiel régional, in M. Pasqualini (ed.), *Les céramiques communes d'Italie et de Narbonnaise. Structures de production, typologies et contextes inédits. IIe s. av. J.-C., IIIe s. apr. J.-C.*, Naples, Centre Jean-Bérard, p. 133-156.

SPEAKMAN R. J., SHACKLEY M. S. (2013) – Silo Science and Portable XRF in Archaeology: a Response to Frahm, *Journal of Archaeological Science*, 40, p. 1435-1443.

STAPFER R., HEITZ C., HINZ M., HAFNER A. (2019) – Interdisciplinary Examinations Carried Out on Heterogeneous Coarse Ceramics from Neolithic Lakeside Settlements in the Northern Alpine Foreland (3900–3500 BCE): Analysis Strategy and Preliminary Results from a Test Series Using pXRF. *Journal of Archaeological Science: Reports*, 25, p. 217-238.

TAYLOR S. R., McLENNAN S. M. (1995) – The Geochemical Evolution of the Continental Crust, *Reviews of Geophysics*, 33, p. 241-265.

TOUTIN-MORIN N., CRÉVOLA G., GIRAULD J. D., BROCARD C., DARDEAU G., BULARD P. F., DUBAR M., MEINESZ A. & BONIJOLY D. (1994) – *Notice explicative, Carte géol. France (1/50000), feuille Fréjus-Cannes (1024)*, Orléans, BRGM, 187 p.

Damase MOURALIS
Université Rouen Normandie, CNRS, IDEES
(UMR6266)
Bâtiment 7c
17, rue Lavoisier
F.-76821 Mont Saint-Aignan cedex
damase.mouralis@univ-rouen.fr
<https://orcid.org/0000-0001-7748-0258>

Chrystèle VERATI
Université Côte d'Azur, CNRS, IRD, OCA,
GÉOAZUR (UMR7329)
Campus Azur
250, rue Albert Einstein
F.-06560 Valbonne
chrystele.verati@univ-cotedazur.fr

Gilles DURRENMATH
Université Côte d'Azur, CNRS, CEPAM
(UMR7264)
MSHS Sud-Est
24, avenue des Diables Bleus
F.-06300 Nice
gilles.durrenmath@univ-cotedazur.fr

Jean-Marc LARDEAUX
Université Côte d'Azur, CNRS, IRD, OCA,
GÉOAZUR (UMR7329)
Campus Azur
250, rue Albert Einstein
F.-06560 Valbonne
jean-marc.lardeaux@univ-cotedazur.fr
and
Center for Lithospheric Research, Czech
Geological Survey, Klárov 3, 11821, Prague 1,
Czech Republic
<https://orcid.org/0000-0001-7666-7109>

Didier BINDER
Université Côte d'Azur, CNRS, CEPAM
(UMR7264)
MSHS Sud-Est
24, avenue des Diables Bleus
F.-06300 Nice
didier.binder@cepam.cnrs.fr
<https://orcid.org/0000-0001-8232-5367>